



Published in final edited form as:

Angew Chem Int Ed Engl. 2015 May 26; 54(22): 6562–6566. doi:10.1002/anie.201411148.

Bridging the Two Worlds: A Universal Interface between Enzymatic and DNA Computing Systems

Shay Mailloux^[b], Dr. Yulia V. Gerasimova^[a], Dr. Nataliia Guz^[b] [Prof.], Dr. Dmitry M. Kolpashchikov^{[a],*}, and Evgeny Katz^{[b],*}

^[a] Chemistry Department, University of Central Florida, 4000 Central, Florida Boulevard, Orlando, FL 32816-2366, USA

^[b] Department of Chemistry and Biomolecular Science, Clarkson University, Potsdam, NY 13699-5810, USA

Abstract

Molecular computing based on enzymes or nucleic acids has attracted a great deal of attention due to the perspectives of controlling living systems in a way we control electronic computers. Enzyme-based computational systems can respond to a great variety of small molecule inputs. They have an advantage of signal amplification and highly specific recognition. DNA computing systems are most often controlled by oligonucleotide inputs/outputs and are capable of sophisticated computing, as well as controlling gene expressions. Here, we developed an interface that enables communication of otherwise incompatible nucleic acid and enzyme computational systems. The enzymatic system processes small molecules as inputs and produces NADH as an output. The NADH output triggers electrochemical release of an oligonucleotide, which is accepted by a DNA computational system as an input. This interface is universal since the enzymatic and DNA computing systems are independent of each other in composition and complexity.

Keywords

Molecular computation; NADH; deoxyribozyme; enzyme computation; electrochemistry

Modern silicon-based analog/digital computer technology has been one of the most successful and influential transformative developments in recent history. At the same time, natural biological molecules (e.g., nucleic acids and proteins) are organized in complex communicating networks responsible for growth of all living creatures through metabolism and reproduction. It was suggested that application of the well-developed computational approach to biological molecules may open new chapters in understanding biological signaling, neuron communication,^[1] and cancer development,^[2] as well as in improving diagnosis of infectious diseases and genetic disorders.^[3] Indeed, biomolecular information processing has been an active research field^[4] in the general framework of chemical^[5]

Dmitry.Kolpashchikov@ucf.edu. ekatz@clarkson.edu.

Supporting information for this article is given via a link at the end of the document.

unconventional computing.^[6] In this research area, DNA computing^[4a-e] and enzyme-based computing^[7] have received exceptional attention. DNA computing is believed to be a potential alternative to electronic computers^[8] for some computational tasks, due to the advantage of massive parallel data processing,^[9] a straightforward design of relatively complex circuits,^[10] and affordability. Among the most obvious applications of DNA-based logic circuits is the analysis of genetic alterations that can be transformed into clinical testing of infectious and genetic diseases.^[2,3] Despite advances in the development of *in vitro* selection, functional DNAs are still limited in the diversity and efficiency of catalytic reactions and are inferior to proteins in terms of affinity and diversity of ligands that DNA can recognize.^[11] At the same time, enzymes are proven to be selective and sensitive receptors; they are known as the best catalysts, enabling rate enhancement up to 10^{17} fold in comparison with uncatalyzed reactions.^[13] However, enzyme-based computing was experimentally limited to the systems mimicking operation of only few concatenated logic gates,^[7] and the network complexity was restricted by enzymes cross-reactivity and noise build.^[14] Combining enzyme and DNA computational systems in communicating enzyme-DNA (Enz/DNA) circuits may enable (i) highly selective recognition of a diverse spectrum of biological molecules or disease markers; (ii) catalytic signal amplification; (iii) massive parallel data processing and (iv) complex computational information processing for biologically generated signals. So far, mixed enzyme-DNA computational systems have been limited to those that involve enzymes directly acting on DNA, e.g., DNA polymerases, DNA ligases, endonuclease, etc.^[15] However, DNA processing enzymes cannot detect such disease biomarkers as small biological molecules, sugars, proteins, etc. On the other hand, biocomputing systems based on general enzymes (not related to DNA) were successfully used for logic processing and binary sensing of various combinations of physiological biomarkers in the YES/NO format.^[16] Therefore, a more universal interface for connecting an enzymatic output signal with DNA-processing circuits is needed. Here, we introduce such an Enz/DNA interface.

The interface recognizes NADH, which is produced as an output of an enzymatic system, and releases a DNA oligonucleotide, which can be processed by a downstream DNA computing system as an input (Figure 1). The interface was based on two modified electrodes (see experimental details in the SI). The first electrode communicating with the enzyme computing system (PQQ-electrode) was coated with adsorbed polyethyleneimine (PEI) and pyrroloquinoline quinone (PQQ) covalently attached to the PEI thin-film.^[17] The immobilized PQQ served as a catalyst for electrochemical oxidation of NADH.^[18] This process resulted in the formation of a negative potential of ca. -60 mV (vs. Ag|AgCl|KCl, 3 M, reference electrode; all other potentials are reported vs. this reference) and the corresponding current sufficient for reduction of Fe^{3+} as part of the Fe^{3+} -cross-linked alginate film on the second connected electrode.^[19] Note that Fe^{2+} cations are not capable of alginate cross-linking, and their formation results in the alginate thin-film dissolution and concomitant release of the entrapped molecules (Figure S1).

In this study we took advantage of two enzyme systems, either of which produced NADH (Figure 2). For binary operation of the enzyme systems, digital input **0** was defined as the absence of the corresponding substrate, whereas digital input **1** was defined as

experimentally optimized concentrations of the substrates. The first system (Figure 2A) operated as a cascade of reactions catalyzed by three enzymes – maltose phosphorylase, hexokinase and glucose-6-phosphate dehydrogenase. It mimicked three concatenated Boolean AND logic gates (Figure 2C), and the high output signal (production of NADH) was observed only in the presence of all four input substrates (see legend to Figure 2). The second system (Figure 2B) operated as a 3-input OR gate connected to an AND gate (Figure 2D). For this system, the NADH production was activated in the presence of any of substrate inputs *A*, *B*, *C* with the mandatory presence of NAD⁺ (input *D*). Enzymatically formed NADH reacted with the PQQ-electrode producing a negative potential and re-oxidized to the NAD⁺ state (Figure 1).

Figure 3 demonstrates the correct digital behavior of the enzymatic logic gate systems interacting with the PQQ-electrode. A negative potential of ca. –60 mV (digital **1**) was achieved when NADH was produced by either of the enzyme logic systems. Otherwise, the potential less negative than –10 mV (digital **0**) was measured (Figure 3). For the enzyme logic system mimicking three concatenated AND gates (Figure 2A,C), logic output **1** (ca. –60 mV) was measured only in the presence of all reacting input species (input combination **1,1,1,1**). All other input combinations (15 different variants) resulted in the electrode potential less negative than –10 mV, digital **0** (Figure 3A). Alternatively, operation of the enzyme system mimicking a 3-input OR gate followed by an AND gate (Figure 2 B,D) resulted in output **1** (ca. –60 mV) generated in the following input combinations (*A,B,C,D*): **0,0,1,1; 0,1,0,1; 1,0,0,1; 0,1,1,1; 1,0,1,1; 1,1,0,1; 1,1,1,1**, while all other input combinations resulted in output signal **0** (Fig. 3B).

To enable transfer of the output signal produced by the enzyme computing systems (Figure 3) into a DNA input signal, the PQQ-electrode was connected to another electrode, which was coated with Fe³⁺-alginate film entrapping a fluorescently labeled DNA oligonucleotide output **OP1** (FITC-5'-TGC AGA CGT TGA AGG ATC CTC). Generation of the negative potential on the PQQ-electrode resulted in subsequent reduction of Fe³⁺ into Fe²⁺ on the Fe³⁺-alginate-coated electrode. It triggered the alginate film dissolution and **OP1** release. It was observed that when the potential of ca. –60 mV (digital **1** output of the enzymatic computing systems) was applied to the second electrode, the alginate film was substantially degraded (Figure S3). At the same time, no visible changes in the film structure were observed at the potential of ca. –5 mV (digital **0** output of the enzyme computing systems), on the same experimental time-scale (data not shown). Fluorescent signal of the solution containing released **OP1** was measured in the presence of different combinations of enzymatic system inputs (Figure 4). As expected, high fluorescence (digital **1**) was registered upon the electrochemically stimulated release of **OP1** in the presence of NADH. When no NADH was produced, the fluorescent signal remained low (digital **0**). The concentration of the released (digital **1**) and leaking (digital **0**) **OP1** was reaching ca. 5 nM and 0.8 nM, respectively, after 30 min. This result shows significant discrimination between the leakage and stimulated release of **OP1** entrapped in the Enz/DNA interface. It should be noted that there is perfect correlation between the output signals produced by the enzymatic systems in the form of the potentials (Figure 3) with the fluorescence of released **OP1**

(Figure 4). In other words, the enzyme-generated output was consistently converted into **OP1**, which served as input for DNA computing as detailed below.

Oligonucleotide **OP1** released by the interface was recognized by a 3-input deoxyribozyme AND gate (**3iAND**) (Figure 5). Deoxyribozyme logic gates controlled by DNA oligonucleotide inputs are most well-developed DNA logic constructs up to date.^[20-22] Indeed, such gates can be assembled in automaton that plays tic-tac-toe game with human,^[20b] they can be organized in multi-layer computational cascades^[21] and a molecular calculator with 7-segment digital display.^[22] The design of **3iAND** takes advantage of the concept of split (binary) deoxyribozyme sensors^[23] and consists of two DNA strands folded in the stem-loop structures (**3iANDa** and **3iANDb** in Figure 5A). The strands are dissociated in the absence of input oligonucleotides. However, hybridization of two oligonucleotide inputs to the loop fragments opens the hairpins and the third input bridges **3iANDa** and **3iANDb**, which results in the formation of a catalytic core (Figure 5B). The deoxyribozyme cleaves a fluorophore- and quencher-labeled substrate (**F substrate** in Figure 5), thus producing high fluorescence. In this study, **OP1**, an output of the Enz/DNA interface, was used as a bridging input for **3iAND**. In experiments with **3iAND** gates, **OP1** without fluorescent label was used. Two other inputs (**I1** and **I2**) mimicked the sequences of microRNAs shown to be promising molecular markers of human cancers.^[24]

According to the truth table (Figure 6A), **3iAND** produces high fluorescence output (digital **1**) only in the presence of all 3 inputs. In our experiments, the **OP1** input was produced *in situ* by the stimulated release (digital **1**) or leakage (digital **0**) from the alginate-modified electrode and its concentration was set by the system as a function of logic operation of the enzyme systems. Two other inputs, **I1** and **I2**, were either used in concentration of 10 nM or absent for digital **1** and **0**, respectively.

The full logic network includes 6 independent logic inputs: 4 inputs (*A, B, C, D*) in the enzyme part and 2 inputs in the DNA part (**I1** and **I2**), while **OP1** is not an independent input. Therefore, the full truth table includes $2^6 = 64$ variants of logic input combinations. Figure 6 shows a simplified representation of the logic process considering only the DNA logic part. Logic value **0** and **1** for the intermediate output/input **OP1** can be realized with various combinations of the enzyme-inputs *A, B, C, D*. For simplicity and for minimizing number of experiments we used *A, B, C, D* enzyme inputs in combinations **0,0,0,0** and **1,1,1,1** for realizing the **OP1** digital values **0** and **1**, respectively. This simplification is justified by very small signal variations of for all combinations of the *A, B, C, D* inputs generating either by output 0 or 1 (Figure 4). In other words, the leakage of **OP1** and the release of **OP1** are almost the same regardless of the input combinations.

The correct digital response of **3iAND** was registered at all possible DNA input combinations (Figure 6B). Importantly, the high output signal (last bar in Figure 6B) could be statistically distinguished from the low output (about 4-fold fluorescence increase, see also Figure S3 for raw fluorescent data). The fluorescent results were supported by the analysis of the samples by gel electrophoresis (Figure S4). The data proves the expected digital response of **3iAND** and the possibility of using an electrode-released oligonucleotide for transferring the signal from enzymatic to DNA computational systems.

This study demonstrates the possibility to design an interface that enables communication between enzymatic and DNA-based computing systems. The whole system includes two individual logic sub-systems (enzyme-based and DNA-based) connected electrically to allow the output signal produced by the enzyme logic gates operate as the input signal for the DNA logic gates. The system operated in two distinct steps, first the enzyme-logic process and then the DNA logic process (see the step-by-step process description in the Supporting Information). To the best of our knowledge, the system reported here is the first Enz/DNA interface that connects a non-DNA processing enzyme computation system with DNA logic gates. We call this interface ‘universal’ because it is compatible with a variety of both enzymatic and DNA molecular logic circuits. NADH communicating between the enzyme system and the interface electrode allows great versatility for the selection of enzymes participating in the biocomputing process, since NADH is produced in a broad variety of reactions. In addition, it is possible to replace NADH with other reducing molecules (e.g., glucose).^[25] The deoxyribozyme gate-based computational systems are also known to show great versatility and complexity.^[20-22] The limitations of the interface are the following. (i) The enzyme-based computing system must produce NADH or other reductive species as an output. (ii) The DNA-based computing system must accept nM-range concentration of oligonucleotide as an input. However, the amount of the released DNA could be increased if larger electrodes or thicker alginate films are used for the DNA entrapment and release. (iii) In its current design, the signal can be transferred in only one direction: from the enzyme to DNA system. (iv) Only one kind of DNA (or a set of DNA sequences) can be released per an electrode pair. More DNA outputs could be released in the controlled way, if a multi-electrode array is applied. Despite the limitations, the reported Enz/DNA system can find some important practical applications. Indeed, the enzymatic and DNA-based computing systems used in this study proved to be relevant to diagnosis of human diseases,^[3,26] as well as to very complex information processing.^[20-22] The reported data represent outputs after the system came to the saturation (the end of the process) similarly to most other studies in the field.^[5f-h,7] It would be interesting to study the time-dependence of output production. The time-dependent outputs were studied experimentally and modelled theoretically for some multi-step biocatalytic reactions applied for logic operations.^[27] Also time-dependent dissolution of alginate thin-film and concomitant release of loaded substances were reported recently.^[28] The present system includes a number of processes with complex kinetics (biocatalytic cascades, electric potential formation, reductive dissolution of alginate, **OPI** release and finally DNA reactions). Study of the combination of these time-dependent processes and their kinetics could become the subject of subsequent investigation. It should be also noted that the alginate film dissolution and subsequent DNA release could be achieved in none-electrochemical systems using direct chemical communication with enzyme logic systems. Similar release processes have been studied using enzyme systems producing citrate as the final output.^[29] However, in this case the choice of potentially useful enzymes is very limited, and EnzDNA interface is not as general as the one reported in this study.

Supplementary Material

Refer to Web version on PubMed Central for supplementary material.

Acknowledgements

This work was supported by the National Institutes of Health (R15AI10388001A1) and NSF CCF (24066076) to DMK and NSF CBET (1403208) to EK.

References

- [1]. a) Qian L, Winfree E, Bruck J. *Nature*. 2011; 475:368–372. [PubMed: 21776082] b) Genot AJ, Fujii T, Rondelez Y. *J. R. Soc. Interface*. 2013; 10:20130212. [PubMed: 23760296] b) Goldental A, Guberman S, Vardi R, Kanter I. *Front. Comput. Neurosci.* 2014; 8:52. [PubMed: 24808856]
- [2]. a) Wang D, Fu Y, Yan J, Zhao B, Dai B, Chao J, Liu H, He D, Zhang Y, Fan C, Song S. *Anal. Chem.* 2014; 86:1932–1936. [PubMed: 24447268] b) Gil B, Kahan-Hanum M, Skirtenko N, Adar R, Shapiro E. *Nano Lett.* 2011; 11:2989–2996. [PubMed: 21671655] c) Hemphill J, Deiters A. *J. Am. Chem. Soc.* 2013; 135:10512–10518. [PubMed: 23795550]
- [3]. a) Konry T, Walt DR. *J. Am. Chem. Soc.* 2009; 131:13232–1323. [PubMed: 19715272] b) Cornett EM, Campbell EA, Gulenay G, Peterson E, Bhaskar N, Kolpashchikov DM. *Angew. Chem. Int. Ed. Engl.* 2012; 51:9075–9077. [PubMed: 22888076] *Angew. Chem.* 2012; 124:9209–9211. c) Gerasimova YV, Kolpashchikov DM. *Chem. Commun.* 2015; 51:870–872.
- [4]. a) Pei R, Matamoros E. *Chem. Commun.* 2015; 51:870–872. Liu M, Stefanovic D, Stojanovic MN. *Nature Nanotechnol.* 2010; 5:773–777. [PubMed: 20972436] b) Stojanovic MN, Stefanovic D, Rudchenko S. *Acc. Chem. Res.* 2014; 47:1845–1852. [PubMed: 24873234] c) Stojanovic MN, Stefanovic D. *J. Comput. Theor. Nanosci.* 2011; 8:434–440. d) Benenson Y. *Nature Rev. Genetics.* 2012; 13:455–468. [PubMed: 22688678] e) Kahan M, Gil B, Adar R, Shapiro E. *Physica D.* 2008; 237:1165–1172. f) Privman V. *Nature Nanotechnol.* 2010; 5:767–768. [PubMed: 21048792] g) Katz, E., editor. *Biomolecular Computing – From Logic Systems to Smart Sensors and Actuators*. Wiley-VCH; Weinheim, Germany: 2012.
- [5]. a) De Silva AP, Uchiyama S, Vance TP, Wannalserse B. *Coord. Chem. Rev.* 2007; 251:1623–1632. b) Szacilowski K. *Chem. Rev.* 2008; 108:3481–3548. [PubMed: 18582117] c) Credi A. *Angew. Chem. Int. Ed.* 2007; 46:5472–5475. *Angew. Chem.* 2007; 119:5568–5572. d) Privman V. *Israel J. Chem.* 2011; 51:118–131. e) Andreasson J, Pischel U. *Chem. Soc. Rev.* 2010; 39:174–188. [PubMed: 20023848] f) Katz, E., editor. *Molecular and Supramolecular Information Processing: From Molecular Switches to Logic Systems*. Wiley-VCH; Weinheim, Germany: 2012. g) Szacilowski, K. *Infochemistry*. Wiley, Chichester; 2012. h) de Silva, AP. *Molecular Logic-Based Computation*. Royal Society of Chemistry; Cambridge: 2013.
- [6]. a) Calude, CS.; Costa, JF.; Dershowitz, N.; Freire, E.; Rozenberg, G., editors. *Lecture Notes in Computer Science*. Vol. 5715. Springer; Berlin: 2009. *Unconventional Computation*. b) Adamatzky, A.; De Lacy Costello, B.; Bull, L.; Stepney, S.; Teuscher, C., editors. *Unconventional Computing*. Luniver Press; Frome, UK: 2007.
- [7]. Katz E, Privman V. *Chem. Soc. Rev.* 2010; 39:1835–1857. [PubMed: 20419221]
- [8]. a) Benenson Y. *Mol. Biosyst.* 2009; 5:675–685. [PubMed: 19562106] b) Stojanovic MN. *Isr. J. Chem.* 2011; 51:99–105.
- [9]. Adleman LM. *Science*. 1994; 266:1021–1024. [PubMed: 7973651]
- [10]. Santini CC, Bath J, Turberfield AJ, Tyrrell AM. *Int. J. Mol. Sci.* 2012; 13:5125–5137. [PubMed: 22606034]
- [11]. a) Schlosser K, Li Y. *Chem. Biol.* 2009; 16:311–322. [PubMed: 19318212] b) Toh SY, Citartan M, Gopinath SC, Tang TH. *Biosens. Bioelectron.* 2014; 64C:392–403. [PubMed: 25278480]
- [13]. Radzicka A, Wolfenden R. *Science*. 1995; 267:90–931. [PubMed: 7809611]
- [14]. a) Privman V, Zavalov O, Halámková L, Moseley F, Haláček J, Katz E. *J. Phys. Chem., B.* 2013; 117:14928–14939. [PubMed: 24205870] b) Privman V, Arugula MA, Haláček J, Pita M, Katz E. *J. Phys. Chem., B.* 2009; 113:5301–5310. [PubMed: 19354308] c) Privman V, Strack G, Solenov D, Pita M, Katz E. *J. Phys. Chem. B.* 2008; 112:11777–11784. [PubMed: 18712917]
- [15]. a) Benenson Y, Paz-Elizur T, Adar R, Keinan E, Livneh Z, Shapiro E. *Nature*. 2001; 414:430–434. [PubMed: 11719800] b) Kolpashchikov DM, Stojanovic MN. *J. Am. Chem. Soc.* 2005; 127:11348–11351. [PubMed: 16089464] c) Han D, Zhu Z, Wu C, Peng L, Zhou L, Gulbakan B,

- Zhu G, Williams KR, Tan W. *J. Am. Chem. Soc.* 2012; 134:20797–20804. [PubMed: 23194304]
- d) Beyer S, Simmel FC. *Nucleic Acids Res.* 2006; 34:1581–1587. [PubMed: 16547201]
- [16]. a) Katz E, Wang J, Privman M, Haláček J. *Anal. Chem.* 2012; 84:5463–5469. [PubMed: 22656194] b) Wang J, Katz E. *Isr. J. Chem.* 2011; 51:141–150. c) Halámková L, Haláček J, Bocharova V, Wolf S, Mulier KE, Beilman G, Wang J, Katz E. *Analyst.* 2012; 137:1768–1770. [PubMed: 22407106] d) Haláček J, Bocharova V, Chinnapareddy S, Windmiller JR, Strack G, Chuang M-C, Zhou J, Santhosh P, Ramirez GV, Arugula MA, Wang J, Katz E. *Molec. Biosys.* 2010; 6:2554–2560.
- [17]. Moore ANJ, Katz E, Willner I. *Electroanalysis.* 1996; 8:1092–1094.
- [18]. Katz E, Lötzbeier T, Schlereth DD, Schuhmann W, Schmidt H-L. *J. Electroanal. Chem.* 1994; 373:189–200.
- [19]. a) Mailloux S, Haláček J, Katz E. *Analyst.* 2014; 139:982–986. [PubMed: 24404562] b) Mailloux S, Guz N, Zakharchenko A, Minko S, Katz E. *J. Phys. Chem. B.* 2014; 118:6775–6784. [PubMed: 24873717] c) Mailloux S, Guz N, Gamella Carballo M, Pingarrón JM, Katz E. *Anal. Bioanal. Chem.* 406. 2014:4825–4829. [PubMed: 24928114] d) Jin Z, Güven G, Bocharova V, Haláček J, Tokarev I, Minko S, Melman A, Mandler D, Katz E. *ACS Appl. Mater. Interfaces.* 2012; 4:466–475. [PubMed: 22200073]
- [20]. a) Stojanovic MN, Mitchell TE, Stefanovic D. *J. Am. Chem. Soc.* 2002; 124:3555–3561. [PubMed: 11929243] b) Stojanovic MN, Stefanovic D. *Nature Biotechnol.* 2003; 21:1069–1074. [PubMed: 12923549] c) Macdonald J, Li Y, Sutovic M, Lederman H, Pendri K, Lu W, Andrews BL, Stefanovic D, Stojanovic MN. *Nano Lett.* 2006; 6:2598–2603. [PubMed: 17090098]
- [21]. a) Stojanovic MN, Semova S, Kolpashchikov D, Macdonald J, Morgan C, Stefanovic D. *J. Am. Chem. Soc.* 2005; 127:6914–6915. [PubMed: 15884910] b) Yashin R, Rudchenko S, Stojanovic MN. *J. Am. Chem. Soc.* 2007; 129:15581–15584. [PubMed: 18031039] c) Brown CW 3rd, Lakin MR, Horwitz EK, Fanning ML, West HE, Stefanovic D, Graves SW. *Angew. Chem. Int. Ed. Engl.* 2014; 53:7183–7187. [PubMed: 24890874] *Angew. Chem.* 2014; 126:7311–7315. d) Brown CW 3rd, Lakin MR, Stefanovic D, Graves SW. *Chembiochem.* 2014; 15:950–954. [PubMed: 24692254]
- [22]. Poje JE, Kastratovic T, Macdonald AR, Guillermo AC, Troetti SE, Jabado OJ, Fanning ML, Stefanovic D, Macdonald J. *Angew. Chem. Int. Ed. Engl.* 2014; 53:9222–9225. [PubMed: 25044570] *Angew. Chem.* 2014; 126:9376–9379.
- [23]. Kolpashchikov DM. *Chembiochem.* 2007; 8:2039–2042. [PubMed: 17924377] (b) Gerasimova YV, Cornett E, Kolpashchikov DM. *Chembiochem.* 2010; 11:811–817. [PubMed: 20301161] (c) Mokany E, Bone SM, Young PE, Doan TB, Todd AV. *J. Am. Chem. Soc.* 2010; 132:1051–1059. [PubMed: 20038095] (d) Gerasimova YV, Kolpashchikov DM. *Chem. Biol.* 2010; 104:106.
- [24]. Liu Z, Sall A, Yang D. *Int. J. Mol. Sci.* 2008; 9:978–999. [PubMed: 19325841]
- [25]. Mailloux S, Haláček J, Halámková L, Tokarev A, Minko S, Katz E. *Chem. Commun.* 2013; 49:4755–4757.
- [26]. a) Gerasimova YV, Cornett EM, Edwards E, Su X, Rohde KH, Kolpashchikov DM. *ChemBioChem.* 2013; 14:2087–2090. [PubMed: 24106198] b) Gerasimova YV, Kolpashchikov DM. *Angew. Chem. Int. Ed. Engl.* 2013; 52:10586–10588. [PubMed: 24038733] *Angew. Chem.* 2013; 125:10780–10782.
- [27]. a) Privman V, Domanskyi S, Mailloux S, Holade Y, Katz E. *J. Phys. Chem. B.* 2014; 118:12435–12443. [PubMed: 25180477] b) Haláček J, Bocharova V, Arugula MA, Strack G, Privman V, Katz E. *J. Phys. Chem. B.* 2011; 115:9838–9845. [PubMed: 21793598]
- [28]. Gamella M, Guz N, Mailloux S, Pingarrón JM, Katz E. *ACS Appl. Mater. Interfaces.* 2014; 6:13349–13354. [PubMed: 25084606]
- [29]. Mailloux S, Zavalov O, Guz N, Katz E, Bocharova V. *Biomaterials Science.* 2014; 2:184–191. Bocharova V, Zavalov O, MacVittie K, Arugula MA, Guz NV, Dokukin ME, Haláček J, Sokolov I, Privman V, Katz E. *J. Mater. Chem.* 2012; 22:19709–19717.

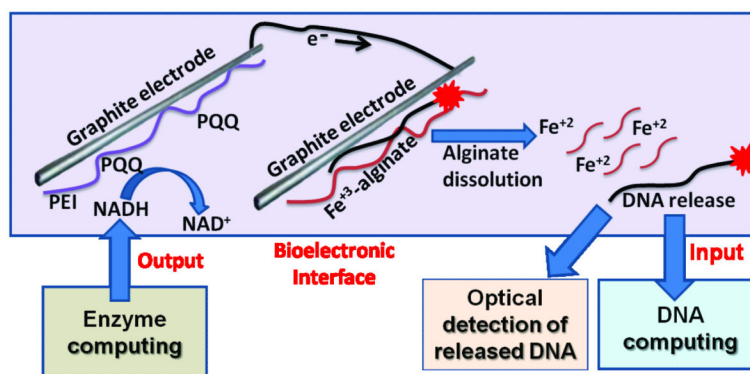


Figure 1. Enzyme computing system produces NADH as an output, which is oxidized on an electrode and reduces Fe³⁺ to Fe²⁺ on another electrode. This leads to dissolution of Fe³⁺-cross-linked alginate polymer and release of an entrapped DNA output. The DNA output can be then used as an input by a DNA computing system.

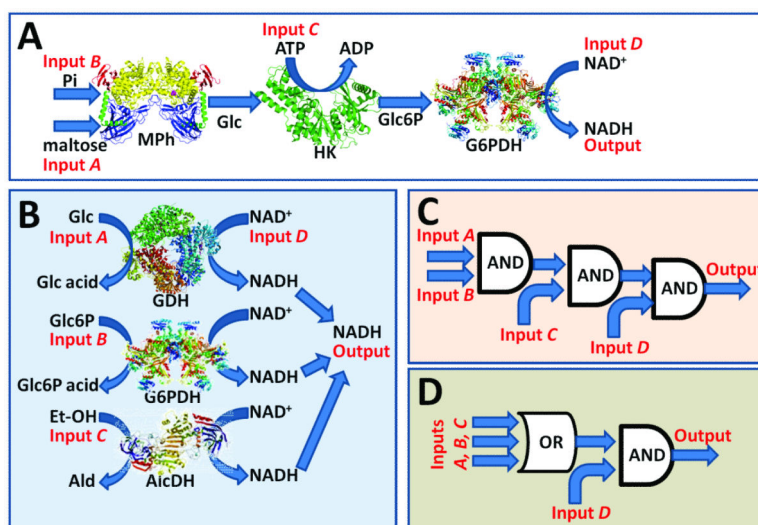


Figure 2.

Two enzyme systems used in this study and their corresponding logic schemes. A) A cascade of three AND gates made of maltose phosphorylase (MPh; E.C. 2.4.1.8), hexokinase (HK; E.C. 2.7.1.1), and glucose-6-phosphate dehydrogenase (G6PDH; E.C. 1.1.1.49). The biocatalytic reaction of MPh was activated in the presence of maltose (input A) and inorganic phosphate (Pi, input B) resulting in glucose (Glc) and glucose-1-phosphate byproduct formation. In the next reaction step catalyzed by HK Glc is converted to glucose-6-phosphate (Glc6P) in the presence of ATP (input C). Finally, Glc6P reduces NAD^+ (Input D) to NADH in the process biocatalyzed by G6PDH. Overall, the NADH production is only possible in the presence of all 4 input signals activating the enzyme-based system. B) A combination of three parallel reactions biocatalyzed by three NAD^+ -dependent enzymes: glucose dehydrogenase (GDH; E.C. 1.1.1.47), G6PDH and alcohol dehydrogenase (AlcDH; E.C. 1.1.1.1). Each biocatalytic reaction was activated by the corresponding substrate: Glc (Input A), Glc6P (Input B) and ethanol (Et-OH), (Input C). The NAD^+ cofactor (input D) was needed for all reactions, thus none of them could proceed in the absence of NAD^+ . C-D) The logic schemes corresponding to the biocatalytic cascades are shown in A and B, respectively.

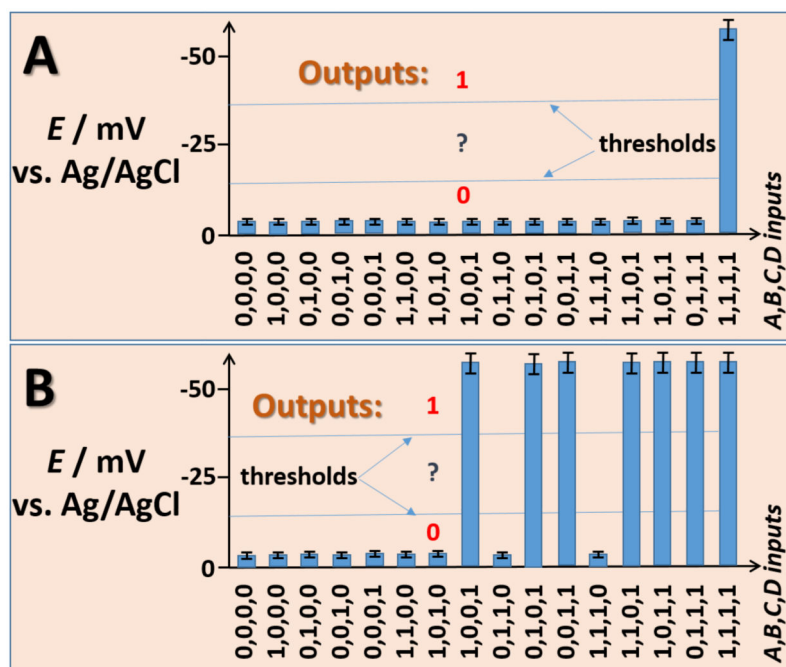


Figure 3.

A-B) Electric potentials generated on the PQQ-modified electrode interfaced with the biocatalytic systems shown in Figures 2A and 2B, respectively, when different combinations of input signals were applied. The bars show the potential values achieved after 30 min of exposing the PQQ-modified electrode to the enzyme systems. The data are average of three independent experiments. The potential produced on the PQQ-modified electrode has a logarithmic dependence on the NADH concentration (according to the Nernst equation), thus resulting in very small variations of the measured potentials. Threshold lines separate logic output **0**, undefined area and logic output **1**.

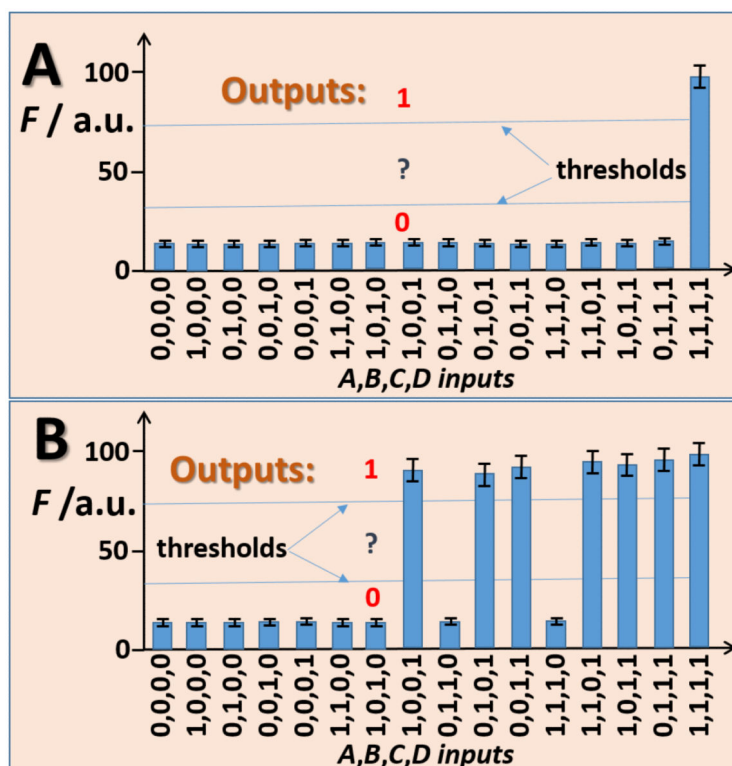


Figure 4.

A-B) Fluorescence signal corresponding to the dye-labelled oligonucleotide **OP1** released from the alginate thin-film when the PQQ-modified electrode was interfaced with the enzymatic logic gate systems shown in Figures 2A and 2B, respectively, when different combinations of input signals were applied. The bars show the fluorescence measured after 30 min of exposing the electrodes to the enzyme systems. The fluorescence is represented by normalized arbitrary values. The data are average of three independent experiments. Threshold lines separate logic output **0**, undefined area and logic output **1**.

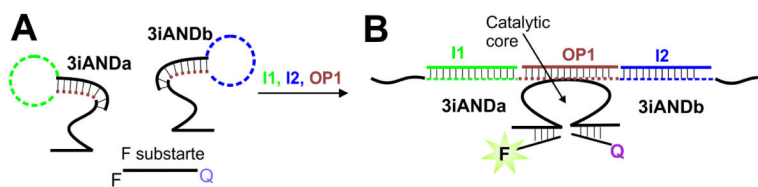


Figure 5.

Principal scheme of a three-input deoxyribozyme AND gate (**3iAND**). **A**) Strands **3iANDa** and **3iANDb** of the gate are dissociated in the absence of inputs. Dashed lines indicate the input-recognition fragments of the strands. **B**) Catalytic Dz complex formed in the presence of all three inputs (**I1**, **OP1**, and **I2**). The Dz catalytic core cleaves the fluorophore- and quencher-labelled F substrate and increases fluorescent signal. Note that **OP1** is not fluorescently labelled.

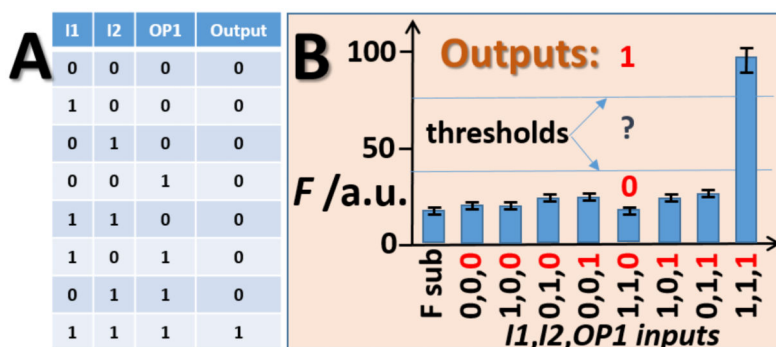


Figure 6.

Digital performance of the **3iAND** gate. A) Truth table; B) Fluorescent response of **3iAND** in the presence of all possible DNA input combinations. The concentrations of the inputs were as follows. For low inputs (digital **0**): **I1**, 0 nM; **I2**, 0 nM; **OP1** was produced *in situ* with the concentration set by the system corresponding to output **0** (when substrate inputs *A,B,C,D* for the enzyme systems were **0,0,0,0**). For high inputs (digital **1**): **I1**, 10 nM; **I2**, 10 nM; **OP1** was produced *in situ* with the concentration set by the system corresponding to output **1** (when inputs *A,B,C,D* for the enzyme systems were **1,1,1,1**). Digital values for **OP1** are shown in red. F sub bar, a control sample containing only fluorescent substrate (**F substrate**, see Figure 5). The bars show the fluorescence measured after 30 min of exposing the electrode to the enzyme systems. The fluorescence is represented by normalized arbitrary values. The data are average of three independent experiments. Threshold lines separate logic output **0**, undefined area and logic output **1**.